THE JOURNAL OF PHYSICAL CHEMISTRY Letters

Letter

Cite This: J. Phys. Chem. Lett. 2019, 10, 4197−4202

pubs.acs.org/JPCL

New Insight into the Photoprotection Mechanism of Plant Sunscreens: Adiabatic Relaxation Competing with Nonadiabatic Relaxation in the *cis* → *trans* Photoisomerization of Methyl Sinapate

Xi Zhao,[†,‡] Jian Luo,[†] Songqiu Yang,[†] and Keli Han*[,†,§]

[†]State Key Laboratory of Molecular Reaction Dynamics, Dalian Institute of Chemical Physics (DICP), Chinese Academy of Sciences, 457 Zhongshan Road, Dalian, Liaoning 116023, China

[‡]University of Chinese Academy of Sciences, Beijing 10049, China

[§]Institute of Molecular Sciences and Engineering, Shandong University, Qingdao 266237, P.R. China

Supporting Information

ABSTRACT: A great deal of thermally instable *cis* form photoisomerization products will be formed from the thermally stable *trans* form of the plant sunscreens sinapate esters upon ultraviolet radiation. To reveal the photoisomerization mechanism of the *cis*-isomer, we explore the photodynamics of a model plant sunscreen methyl sinapate (MS) in the *cis* form in organic solution. The high photoisomerization quantum yield of the *cis*-isomer results in the relatively higher photostability of *trans*-MS. By utilizing femtosecond transient absorption spectroscopy and quantum chemical calculation, we propose that an adiabatic relaxation competes with nonadiabatic relaxation for the excited-state *cis* form of methyl sinapate. These results suggest that the photoprotection mechanism of the *cis* form of sinapate esters is significantly different from that of the *trans* form of sinapate esters and plays an important role in the overall photoprotection effect.

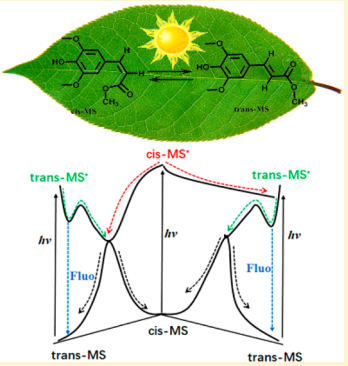

Various sunscreens such as oxybenzone[1] and cinnamate-based molecules[2−4] have been used to protect against overexposure to ultraviolet (UV) radiation. Sinapoyl malate is a natural sunscreen for photoprotection that is deposited in the leaves of *Arabidopsis* plants.[5−7] Although the photodynamics of sinapate esters have been comprehensively studied, researchers mainly focus on the *trans*-isomer, which is the naturally produced form.[8−12] In general, a quantity of *cis*-sinapate esters will be formed from *trans*-isomers after a long time exposure to UV radiation,[8,10,11] and the photochemistry of these *cis*-isomers may play an important role in the overall photoprotection effect. Because of the difficulties in directly synthesizing the *cis*-isomer of these sinapate esters, the photoinduced *cis*-isomer product has been ignored and few studies have been done.[13] Therefore, further study on the *cis*-isomer of sinapate esters is an urgent need.

In this Letter, we explore the photoprotection mechanism of a model plant sunscreen in the *cis* form and compare that with the *trans* form. Because the size of the ester functional group has little effect on the photochemistry of the sinapate esters,[8,11,12] we synthesized the methyl sinapate (MS), the most simple sinapate ester whose photoprotection capability is similar to that of the natural sunscreen sinapoyl malate.[8,10,12] Moreover, the *cis*-isomer of MS is obtained by thin-layer chromatography (TLC). The photoisomerization of *trans* ↔ *cis* is shown in Scheme 1. In the present work, the photoisomerization quantum yields of the *cis* and *trans* forms of MS are obtained. The significant high photoisomerization quantum yield of the *cis*-isomer results in a relatively higher photostability of *trans*-MS. Moreover, we confirm that the fluorescence of the *cis*-isomer originates from the excited state of the *trans*-isomer. Finally, we first propose that there is an adiabatic relaxation that competes with nonadiabatic relaxation for the excited-state *cis*-isomer.

The steady-state ultraviolet−visible (UV−vis) absorption and fluorescence spectra of *cis*-MS and *trans*-MS in methanol are shown in Figure 1. Both *cis* and *trans* isomers have a large absorption section in the UV region. The peak of the absorption spectrum of *trans*-MS (326 nm) is slightly redshifted in comparison to that of *cis*-MS. The molar extinction coefficient of *trans*-MS is higher than that of *cis*-MS,[13,14] implying the better photoprotection effect of *trans*-MS.

The fluorescence spectra of *trans* and *cis* isomers are both peaked at approximately 440 nm; it is clear that the fluorescence spectra shape of *trans*-MS and *cis*-MS are similar. As shown in Table 1, the fluorescence quantum yield of *trans*-MS is about 2.5 times larger than that of *cis*-MS. The smaller fluorescence quantum yield of *cis*-MS indicates the nonradiative decay of *cis*-MS is easier than that of the *trans*-MS. The emission spectra of these two isomers at 77 K are no longer the same, as shown in Figure 1b. The temperature-

Received: June 7, 2019
Accepted: July 9, 2019
Published: July 9, 2019

DOI: 10.1021/acs.jpclett.9b01651
J. Phys. Chem. Lett. 2019, 10, 4197−4202

Scheme 1. Photoisomerization between *trans*-Methyl Sinapate (*trans*-MS) and *cis*-MS

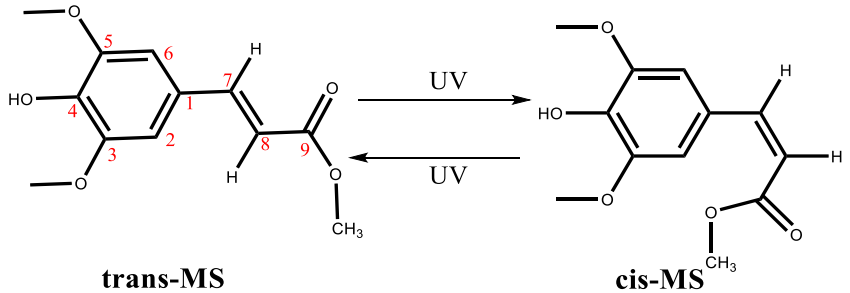

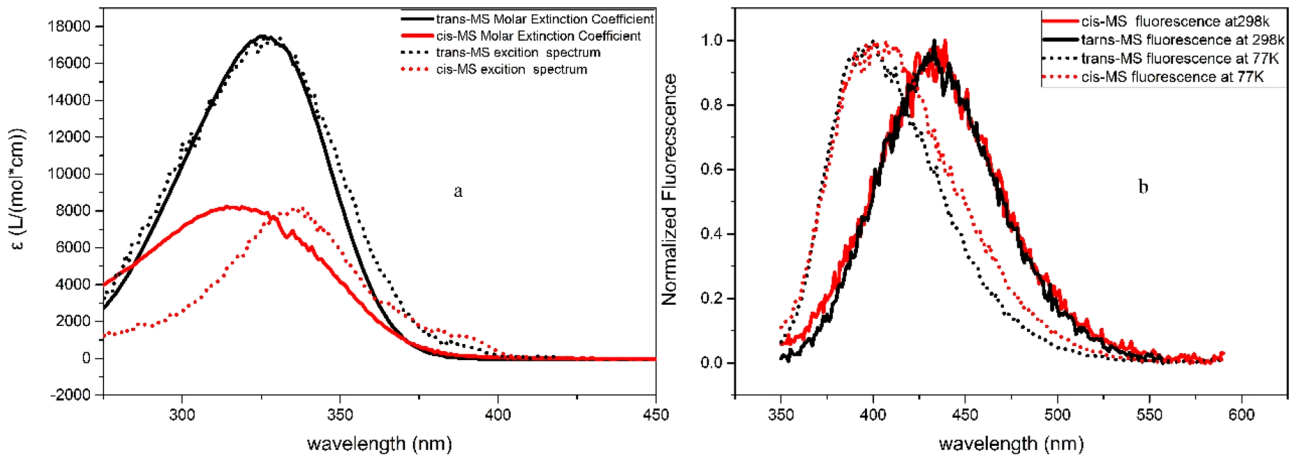

Figure 1. Steady-state absorption (a) and normalized fluorescence (b) spectra of *trans*-MS (black solid line) and *cis*-MS (red solid line) in MeOH at room temperature. The excitation spectra of *trans*-MS (black dotted line) and *cis*-MS (red dotted line) at room temperature are shown in panel a; the intensity of the excitation spectra is scaled for comparison. The emission spectra of *trans*-MS (black dotted line) and *cis*-MS (red dotted line) at 77 K are shown in panel b for comparison.

Table 1. Fluorescence Quantum Yields, Barrier on the Excited-State Potential Energy Surface, and the Photoisomerization Quantum Yield of *trans*-MS and *cis*-MS

structure	Φ_{fl} ($\times 10^3$)	$\triangle G$ (kcal/mol)	Φ_{iso}
trans-MS	5.1	2.7	0.22
cis-MS	2.1	2.9	0.77

dependent emission behavior of *trans*-MS and *cis*-MS indicates fluorescence emission of *cis*-MS may result from excited *trans*-MS*, which implies an adiabatic *cis*-MS* → *trans*-MS* isomerization has occurred.[15] Because the temperature is lower than the melting point of methanol, a torsional barrier was introduced by the low temperature. The solvent relaxation rate may be much slower, and the emission at 77 K is assigned from the region around the Franck−Condon region. This is consistent with the dramatic blue shift (about 50 nm) of the emission spectra at 77 K shown in Figure 1. The excitation spectra of *trans*-MS and *cis*-MS at room temperature are shown in Figure 1a. The shapes of the absorption spectrum and excitation spectrum for *trans*-MS are quite similar; both peak at 326 nm. However, the excitation spectrum of *cis*-MS shows an obvious red shift (18 nm) relative to the corresponding absorption spectrum, suggesting the difference between excited *trans*-MS* precursors and excited *cis*-MS* precursors.

The temperature-dependent fluorescence quantum yield was employed to estimate the isomerization barrier energy of *trans*-MS and *cis*-MS on the excited-state potential energy surface (PES). Fluorescence quantum yields at 283−325 K were measured (Figure S1). The isomerization barrier of *cis*-MS in the excited state, shown in Table 1, is evaluated to be 2.9 kcal/mol, similar to that of *trans*-MS (2.7 kcal/mol). The similar fluorescence spectrum at room temperature but the difference at 77 K, the difference of excitation spectrum at room temperature, and the similar isomerization barrier obtained through the temperature-dependent fluorescence between these two isomers indicate the fluorescence of both isomers may originate from *trans*-MS*. Thus, the isomerization barrier of *cis*-MS in the excited state may stem from the isomerization process of *trans*-MS in the excited state, which is formed adiabatically from the *cis*-MS*.

The quantum yields of the photoisomerization process of *trans*-MS and *cis*-MS were measured in methanol, as summarized in Table 1. The substantial overlap of the absorption spectra of these two isomers results in a photostationary state (PSS) upon irradiation with UV light. The changing absorption spectrum of *trans*-MS in methanol is shown in Figure S2. It is clear to see that a PSS is achieved because there is no further change in the absorption spectrum. Furthermore, ^{1}H NMR spectra of *trans*-MS and *cis*-MS in methanol-d_4 with UV radiation were measured (Figures S5 and S6), ensuring that the photoisomerization is only between *trans*-MS and *cis*-MS when irradiated with UV light. The quantum yield of *cis* → *trans* isomerization is 3.5 times higher than the corresponding reverse photoisomerization reaction (0.77 vs 0.22). Because of the higher quantum yield of *cis* → *trans* isomerization compared to the reversible isomerization process in excites-state, the ratio of *trans*-MS would be higher in the photostationary state. The absorption efficiency of *trans*-

DOI: 10.1021/acs.jpclett.9b01651
J. Phys. Chem. Lett. 2019, 10, 4197−4202

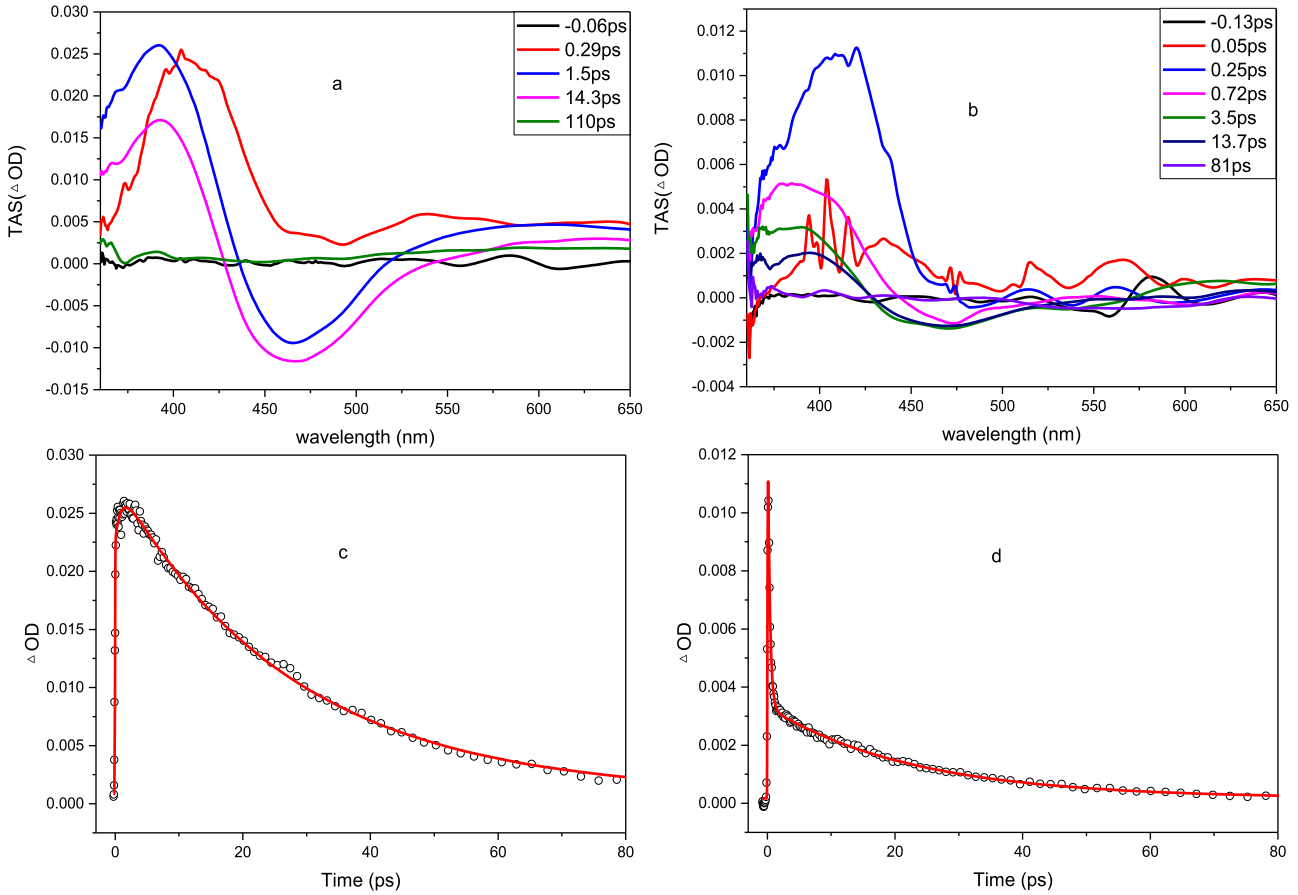

Figure 2. Femtosecond wavelength evolution curves of (a) *trans*-MS and (b) *cis*-MS at 320 nm pulse. Excited-state absorption decays of *trans*-MS (c) and *cis*-MS (d) at 395 nm. The experimental data are shown in circles, and the fitted results are shown in solid lines.

Table 2. Summary of the Excited-State Lifetime of *trans*-MS and *cis*-MS in Methanol

	a_1	τ_1 (ps)	a_2	τ_2 (ps)
trans-MS	−0.002 ± 0.0002	0.92 ± 0.24	0.01 ± 0.0001	27.7 ± 0.9
cis-MS	0.006 ± 0.003	0.32 ± 0.023	0.0016 ± 0.0001	22.8 ± 2.1

MS in the UV region is stronger than that of *cis*-MS; thus, the high photoisomerization quantum yield of *cis* → *trans* isomerization results in relatively higher photostability of MS when irradiated with UV light,[12] illustrating the good performance of MS as a sunscreen.

The evolution of the transient absorption spectrum in methanol measured by FTA spectroscopy is shown in Figure 2. As shown in Figure 2a, the evolution of the transient absorption spectrum of *trans*-MS* is dominated by an excited-state absorption (ESA) band peak around 390 nm and a stimulated emission (SE) peak around 465 nm, evidenced by the steady-state emission centered at 440 nm (Figure 1b). In the early delay stage, there is a slight blue shift of the ESA band with a drop in intensity following 320 nm femtosecond pulse excitation. This is ascribed to the excited-state vibrational relaxation (VR) and solvent relaxation.[8,10] The evolution of the transient absorption spectrum of *cis*-MS* (Figure 2b) is also dominated by an ESA band and an SE band. The slight blue shift of the ESA band indicates excited-state VR and solvent relaxation of *cis*-MS*. At early relaxation times, the decay of the ESA band of *cis*-MS* is obviously faster than that of *trans*-MS* and the intensity of the ESA band is significantly stronger than the intensity of the SE band when compared with that of *trans*-MS*. For clarity, a biexponential function is used to fit the decay kinetics of these two isomers around the peak of the ESA band (Figure 2c,d), resulting in one short subpicosecond lifetime and another long picosecond lifetime, summarized in Table 2. For *trans*-MS, the τ_1 (0.92 ps) with a negative pre-exponential factor is assigned as the comprehensive results of VR, solvent relaxation, and other nonequilibrium process, while the τ_2 (27.7 ps) with a positive pre-exponential factor is assigned to the *trans*−*cis* isomerization process on the excited-state PES.[8,16] For *cis*-MS, it is clear that there is a fast subpicosecond decay (τ_1, 0.32 ps) of the ESA band followed by a slow ESA band decay (τ_2, 22.8 ps). It should be noted that the pre-exponential factors for both processes are positive; moreover, the value of the pre-exponential factor for the fast decay process is about four times larger than that of the slow decay process, which is different from that of *trans*-MS*. When the two lifetimes of *trans*-MS* and *cis*-MS* are compared, the subpicosecond lifetime of *cis*-MS* is much less than that of *trans*-MS* (0.32 ps vs 0.9 ps) and the sign of the pre-exponential factor is different, which indicates that the subpicosecond lifetime of *cis*-MS* cannot be assigned to VR or solvent relaxation; the longer lifetimes of *cis*-MS* and *trans*-MS* are quite similar (27.7 ps vs 22.8 ps). The subpicosecond

DOI: 10.1021/acs.jpclett.9b01651
J. Phys. Chem. Lett. 2019, 10, 4197−4202

lifetime of *cis*-MS* with a relatively large pre-exponential factor is reasonably assigned to the decay of *cis*-MS*, and it is safe to consider that the fluorescence from *cis*-MS* can be ignored because of the ultrafast decay of the *cis*-MS* (0.3 ps). The longer lifetime of about 23 ps of *cis*-MS* is assigned to the decay of *trans*-MS* because of the similarity of the lifetime with *trans*-MS*.

According to the experimental results of FTA spectroscopy and fluorescence, the subpicosecond lifetime is assigned to the decay of *cis*-MS* and the long lifetime component of biexponential fit is assigned to the decay of *trans*-MS*, which is formed adiabatically from the *cis*-MS*. Thus, the isomerization barrier of *cis*-MS in the excited state obtained from the temperature-dependent fluorescence experiment actually stems from the isomerization barrier for the C=C double bond twisting of *trans*-MS* in the excited-state. This is in accord with the similar fluorescence spectra and isomerization barriers of these two isomers. All these experimental results indicate that the fluorescence of *cis*-MS* originates from the *trans*-MS* and that an adiabatic relaxation of *cis*-MS* to *trans*-MS* is occurring.

Quantum chemical calculations were employed to give a deep insight into the photoisomerization process of these two isomers. As shown in Scheme 1, MS is constructed with a phenyl ring and a methyl acrylate. The phenyl ring is connected with an acrylic double bond by a flexible C_1-C_7 single bond. The rotation around the C_1-C_7 single bond is described by α, defined as the $C_2C_1C_7C_8$ dihedral angle, and the $C_7=C_8$ double bond twisting is described by β, defined as the $C_1C_7C_8C_9$ dihedral angle. The equilibrium structures of *trans*-MS and *cis*-MS are obtained at the M062X/6-31+g-(d,p)[17,18] calculation level, as shown in Figure S3. For ground-state equilibrium *trans*-MS, $\alpha = 0°$ and $\beta = 180°$ (Figure S3a) indicate the coplanar phenyl ring and the double C=C bond. In contrast, for *cis*-MS, the $\alpha = -34°$ and $\beta = -5°$ (Figure S3b) indicate that there is a significant rotation around the C_1-C_7 single bond resulting from the steric repulsion between the phenyl ring and the substituted ester group. The vertical excitation energies of these two isomers are shown in Table 3.

Table 3. Vertical Excitation Energies (eV) and Oscillator Strengths (in Parentheses) of the Two Lowest Excited States (S_1 and S_2) in Methanol Solution at the TD-M062X/6-31+g(d,p) Level of Theory[a]

energy	*trans*-MS	*cis*-MS
exptl	3.80	3.91
S_1	4.10 (0.72)	4.26 (0.37)
S_2	4.55 (0.03)	4.69 (0.02)

[a]The experimental absorption energies are also shown for comparison.

Photoexcitation around 320 nm leads to a $1^1\pi\pi^* \leftarrow S_0$ transition.[6] The calculated absorption energy sequence and oscillator strengths of these two isomers are consistent with the experimental results shown in Figure 1. Further details about quantum chemical calculations can be found in the Supporting Information. According to numerous literature contributions on cinnamates,[2,3,11,13,14,16,19−21] the C=C bond twisting is the main reaction coordinate that drives the excited-state species to a conical intersection. After passing through the conical intersection, the molecules can either go back to the *trans*-reactant or forward to the *cis*-product.

We located the optimized structure around the Franck−Condon region in the S_1 state of *trans*-MS and a corresponding transition-state structure in the photoisomerization reaction coordinate, as shown in Figure S4. The optimized structure in the S_1 state has a similar configuration with the Franck−Condon point characterized with $\alpha = 0°$ and $\beta = 180°$. For the transition state in the S_1 state, the calculated barrier for photoisomerization is 3.1 kcal/mol, which is in accordance with the experimental result. Moreover, for the transition-state structure, $\alpha = -2.0°$ and $\beta = -129°$, the significant rotation of the $C_1C_7C_8C_9$ dihedral angle is consistent with the hypothesis that C=C bond twisting is the main reaction coordinate. The conical intersection structure connecting the excited and ground states of MS in methanol solution is located with the help of the Firefly package,[22,23] as shown in Figure S4c, characterized with $\alpha = 1°$ and $\beta = -94°$. The coplanar between $C_7{=}C_8$ double bond and phenyl ring and the significant $C_7{=}C_8$ double bond twisting in the conical intersection indicate $C_7{=}C_8$ double bond twisting drives the excited state to the conical intersection. Thus, we propose the relaxation scheme of *trans*-MS* as shown in Figure 3. *trans*-MS was populated to

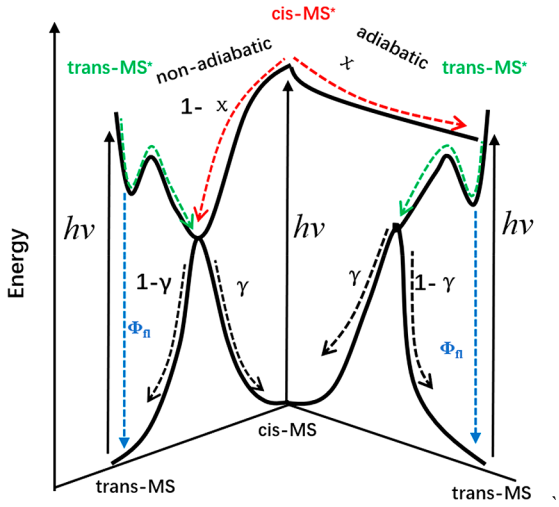

Figure 3. Schematic of the relaxation scheme of MS molecules proposed in this work.

the S_1 state upon excitation with UV light, and an excited equilibrium state is reached after an ultrafast relaxation from the Franck−Condon region. This excited equilibrium state corresponds to the fluorescence from *trans*-MS*. After a barrier is overcome along with the C=C bond twisting in the excited state, a $1^1\pi\pi^*/S_0$ conical intersection is reached where a nonadiabatic relaxation occurs. In particular, after relaxation through the conical intersection, the hot molecules can either go back to the *trans*-reactant or forward to the *cis*-product. The branch ratio between reactant and product through the conical intersection can be determined by the fluorescence quantum yield in company with the photoisomerization quantum yield of *trans*-MS (shown in the Supporting Information). The branch ratio is 0.787 for *trans*-reactant formation and 0.213 for *cis*-product formation, similar to previous work in which the excited states are deactivated by C=C bond rotation.[24]

Note that there is no optimized structure for *cis*-MS in the S_1 state, indicating the barrierless isomerization process in the lowest excited state. TD-M062X[17,18] is employed to construct the PES by linearly interpolating internal coordinates (LIIC)

DOI: 10.1021/acs.jpclett.9b01651
J. Phys. Chem. Lett. 2019, 10, 4197−4202

between S_0 and conical intersection geometries. As shown in Figure S7, the descent trends from the FC region to the conical intersection is consistent with the absence of an optimized structure. The barrierless isomerization corresponds to the subpicosecond lifetime of *cis*-MS*. As the molecular structure of *cis*-MS* evolves along the S_1 PES, the C_1-C_8 single bond has a significant rotation, as evidenced by its α increasing from −34° in the Franck−Condon region to 1° in the conical intersection. Given that β also decreases from −5° in the Franck−Condon region to −94° in the conical intersection, a combination of single-bond and double-bond rotations occurs in the relaxation of *cis*-MS*, which is known as the famous hula twist.[25−29] The steric repulsion between the phenyl ring and the substituted ester group of *cis*-MS, which is absent in the *trans*-MS isomer, leads to a pretwisting structure and the hula twist reaction coordinate in the excited state, contributing to the barrierless relaxation.

As has been determined, the temperature-dependent fluorescence quantum yield and FTA experiment of *cis*-MS indicate an adiabatic *cis*-MS* to *trans*-MS* isomerization. The barrierless hula twist of *cis*-MS leads the excited-state molecules to a conical intersection incapable of explaining the fluorescence of *cis*-MS, which is determined to originate from the *trans*-MS*. Herein, we propose that there is an adiabatic relaxation competing with the nonadiabatic relaxation for *cis*-MS*. In comparison with *trans*-MS*, the relatively weak SE intensity of *cis*-MS* when compared with the intensity of ESA band suggests only a portion of *cis*-MS* transformed into *trans*-MS*, which is consistent with our proposal. The portion of molecules undergoing adiabatic relaxation can be estimated by the fluorescence quantum yield of *cis*-MS based on the assumption that the fluorescence from *cis*-MS* is solely from the *trans*-MS*. The ultrafast subpicosecond decay of *cis*-MS* ensures the rationality of ignoring the fluorescence from *cis*-MS*. The ratio between adiabatic relaxation and nonadiabatic relaxation is 41:59 according to the fluorescence quantum yield of these two isomers. Forty one percent of the first populated *cis*-MS* molecules evolved to the *trans*-MS* through an adiabatic isomerization and then decayed to the ground state as previously described for *trans*-MS*. In the meantime, the other portion of the initially populated *cis*-MS* molecules were deactivated to the ground state along a barrierless hula twist and passed through a conical intersection. Furthermore, the photoisomerization quantum yield of *cis*-MS can be estimated based on the relaxation scheme we proposed, which is determined to be 0.78 (shown in the Supporting Information) and is in agreement with the experimental result of 0.77, as shown in Table 1. The consistency of these two photoisomerization quantum yields obtained by different methods indicates the validity of the scheme shown in Figure3.

In conclusion, we have explored the photoprotection mechanism of a model plant sunscreen MS in *cis* and *trans* forms. The present work serves to highlight the difference between these two isomers in the photoisomerization mechanism. The relatively high photoisomerization quantum yield of the *cis*-isomer results in a high photostability of *trans*-MS. We suggest, for the thermally stable *trans*-MS, a nonadiabatic relaxation occurs on the excited PES where a conical intersection is reached after a barrier is overcome along the C=C double bond twisting. This work also reveals that the fluorescence of *cis*-MS stems from *trans*-MS* and suggests an adiabatic relaxation competing with a nonadiabatic relaxation for the thermally instable *cis*-MS. We further reveal that the steric repulsion in *cis*-MS promotes a hula twist in the excited-state relaxation. These results reveal the difference between *trans*- and *cis*-MS in photodynamics and give further insight into the photoprotection mechanism of plant sunscreens.

■ ASSOCIATED CONTENT

Supporting Information

The Supporting Information is available free of charge on the ACS Publications website at DOI: 10.1021/acs.jpclett.9b01651.

Synthesis of studied molecules, photoisomerization quantum yield of both isomers, temperature-dependent fluorescence yields, computational details, optimized ground-state geometries, and continuous UV irradiation ^{1}H NMR spectra (PDF)

■ AUTHOR INFORMATION

Corresponding Author

*E-mail: klhan@dicp.ac.cn.

ORCID

Jian Luo: 0000-0002-3928-793X

Keli Han: 0000-0001-9239-1827

Notes

The authors declare no competing financial interest.

■ ACKNOWLEDGMENTS

The work is supported by the National Natural Science Foundation of China (Nos. 21833009, 21533010, 21703244, and 21403226), the National Key Research and Development Program of China (Grant Nos. 2016YFE0120900 and 2017YFA0204800), DICP DMTO201601, DICP ZZBS201703, and the Science Challenging Program (JCKY2016212A501).

■ REFERENCES

(1) Baker, L. A.; Horbury, M. D.; Greenough, S. E.; Coulter, P. M.; Karsili, T. N. V.; Roberts, G. M.; Orr-Ewing, A. J.; Ashfold, M. N. R.; Stavros, V. G. Probing the Ultrafast Energy Dissipation Mechanism of the Sunscreen Oxybenzone after UVA Irradiation. *J. Phys. Chem. Lett.* **2015**, *6*, 1363−1368.

(2) Tan, E. M. M.; Hilbers, M.; Buma, W. J. Excited-State Dynamics of Isolated and Microsolvated Cinnamate-Based UV-B Sunscreens. *J. Phys. Chem. Lett.* **2014**, *5*, 2464−2468.

(3) Miyazaki, Y.; Inokuchi, Y.; Akai, N.; Ebata, T. Direct Spectroscopic Evidence of Photoisomerization in para-Methoxy Methylcinnamate Revealed by Low-Temperature Matrix-Isolation FTIR Spectroscopy. *J. Phys. Chem. Lett.* **2015**, *6*, 1134−1139.

(4) Chang, X.-P.; Li, C.-X.; Xie, B.-B.; Cui, G. Photoprotection Mechanism of p-Methoxy Methylcinnamate: A CASPT2 Study. *J. Phys. Chem. A* **2015**, *119*, 11488−11497.

(5) Chapple, C. C.; Vogt, T.; Ellis, B. E.; Somerville, C. R. An Arabidopsis mutant defective in the general phenylpropanoid pathway. *Plant Cell* **1992**, *4*, 1413−1424.

(6) Ruegger, M.; Chapple, C. Mutations That Reduce Sinapoylmalate Accumulation in Arabidopsis thaliana Define Loci With Diverse Roles in Phenylpropanoid Metabolism. *Genetics* **2001**, *159*, 1741−1749.

(7) Fraser, C. M.; Chapple, C. The Phenylpropanoid Pathway in Arabidopsis. *The Arabidopsis Book* **2011**, *9*, e0152.

(8) Baker, L. A.; Horbury, M. D.; Greenough, S. E.; Allais, F.; Walsh, P. S.; Habershon, S.; Stavros, V. G. Ultrafast Photoprotecting Sunscreens in Natural Plants. *J. Phys. Chem. Lett.* **2016**, *7*, 56−61.

(9) Dean, J. C.; Kusaka, R.; Walsh, P. S.; Allais, F.; Zwier, T. S. Plant Sunscreens in the UV-B: Ultraviolet Spectroscopy of Jet-Cooled

DOI: 10.1021/acs.jpclett.9b01651
J. Phys. Chem. Lett. 2019, 10, 4197−4202

Sinapoyl Malate, Sinapic Acid, and Sinapate Ester Derivatives. *J. Am. Chem. Soc.* **2014**, *136*, 14780−14795.
(10) Luo, J.; Liu, Y.; Yang, S.; Flourat, A. L.; Allais, F.; Han, K. Ultrafast Barrierless Photoisomerization and Strong Ultraviolet Absorption of Photoproducts in Plant Sunscreens. *J. Phys. Chem. Lett.* **2017**, *8*, 1025−1030.
(11) Horbury, M. D.; Quan, W. D.; Flourat, A. L.; Allais, F.; Stavros, V. G. Elucidating nuclear motions in a plant sunscreen during photoisomerization through solvent viscosity effects. *Phys. Chem. Chem. Phys.* **2017**, *19*, 21127−21131.
(12) Liu, Y.; Zhao, X.; Luo, J.; Yang, S. Excited-state dynamics of sinapate esters in aqueous solution and polyvinyl alcohol film. *J. Lumin.* **2019**, *206*, 469−473.
(13) Horbury, M. D.; Flourat, A. L.; Greenough, S. E.; Allais, F.; Stavros, V. G. Investigating isomer specific photoprotection in a model plant sunscreen. *Chem. Commun.* **2018**, *54*, 936−939.
(14) Hanson, K. M.; Narayanan, S.; Nichols, V. M.; Bardeen, C. J. Photochemical degradation of the UV filter octyl methoxycinnamate in solution and in aggregates. *Photochem. Photobiol. Sci.* **2015**, *14*, 1607−1616.
(15) Sun, W.-T.; Huang, G.-J.; Huang, S.-L.; Lin, Y.-C.; Yang, J.-S. A Light-Gated Molecular Brake with Antilock and Fluorescence Turn-On Alarm Functions: Application of Singlet-State Adiabatic Cis → Trans Photoisomerization. *J. Org. Chem.* **2014**, *79*, 6321−6325.
(16) Wang, S.; Schatz, S.; Stuhldreier, M. C.; Böhnke, H.; Wiese, J.; Schröder, C.; Raeker, T.; Hartke, B.; Keppler, J. K.; et al. Ultrafast dynamics of UV-excited trans- and cis-ferulic acid in aqueous solutions. *Phys. Chem. Chem. Phys.* **2017**, *19*, 30683−30694.
(17) Zhao, Y.; Truhlar, D. G. The M06 suite of density functionals for main group thermochemistry, thermochemical kinetics, noncovalent interactions, excited states, and transition elements: two new functionals and systematic testing of four M06-class functionals and 12 other functionals. *Theor. Chem. Acc.* **2008**, *120*, 215−241.
(18) Zhao, Y.; Truhlar, D. G. Density Functionals with Broad Applicability in Chemistry. *Acc. Chem. Res.* **2008**, *41*, 157−167.
(19) Peperstraete, Y.; Staniforth, M.; Baker, L. A.; Rodrigues, N. D. N.; Cole-Filipiak, N. C.; Quan, W.-D.; Stavros, V. G. Bottom-up excited state dynamics of two cinnamate-based sunscreen filter molecules. *Phys. Chem. Chem. Phys.* **2016**, *18*, 28140−28149.
(20) Horbury, M. D.; Baker, L. A.; Quan, W.-D.; Greenough, S. E.; Stavros, V. G. Photodynamics of potent antioxidants: ferulic and caffeic acids. *Phys. Chem. Chem. Phys.* **2016**, *18*, 17691−17697.
(21) Miyazaki, Y.; Yamamoto, K.; Aoki, J.; Ikeda, T.; Inokuchi, Y.; Ehara, M.; Ebata, T. Experimental and theoretical study on the excited-state dynamics of ortho-, meta-, and para-methoxy methyl-cinnamate. *J. Chem. Phys.* **2014**, *141*, 244313.
(22) Schmidt, M. W.; Baldridge, K. K.; Boatz, J. A.; Elbert, S. T.; Gordon, M. S.; Jensen, J. H.; Koseki, S.; Matsunaga, N.; Nguyen, K. A.; Su, S.; et al. General atomic and molecular electronic structure system. *J. Comput. Chem.* **1993**, *14*, 1347−1363.
(23) Granovsky, A. A. *Firefly*, version 8; http://classic.chem.msu.su/gran/firefly/index.html.
(24) Polli, D.; Altoè, P.; Weingart, O.; Spillane, K. M.; Manzoni, C.; Brida, D.; Tomasello, G.; Orlandi, G.; Kukura, P.; Mathies, R. A.; et al. Conical intersection dynamics of the primary photoisomerization event in vision. *Nature* **2010**, *467*, 440.
(25) Calipari, E. S.; Godino, A.; Peck, E. G.; Salery, M.; Mervosh, N. L.; Landry, J. A.; Russo, S. J.; Hurd, Y. L.; Nestler, E. J.; Kiraly, D. D. Granulocyte-colony stimulating factor controls neural and behavioral plasticity in response to cocaine. *Nat. Commun.* **2018**, *9*, 9.
(26) Liu, Y.; Luo, J. Nonadiabatic dynamics simulation of photoisomerization mechanism of photoswitch azodicarboxamide: Hydrogen bonding effects. *J. Photochem. Photobiol., A* **2018**, *367*, 236−239.
(27) Fuß, W.; Kosmidis, C.; Schmid, W. E.; Trushin, S. A. The Photochemical cis−trans Isomerization of Free Stilbene Molecules Follows a Hula-Twist Pathway. *Angew. Chem., Int. Ed.* **2004**, *43*, 4178−4182.
(28) Fuß, W. Hula-twist cis−trans isomerization: The role of internal forces and the origin of regioselectivity. *J. Photochem. Photobiol., A* **2012**, *237*, 53−63.
(29) Liu, R. S. H. Photoisomerization by Hula-Twist: A Fundamental Supramolecular Photochemical Reaction. *Acc. Chem. Res.* **2001**, *34*, 555−562.

DOI: 10.1021/acs.jpclett.9b01651
J. Phys. Chem. Lett. 2019, 10, 4197−4202